Practical Flow Cytometry in Haematology

100 Worked Examples

Mike Leach
Mark Drummond
Allyson Doig
Pam McKay
Bob Jackson
Barbara J. Bain

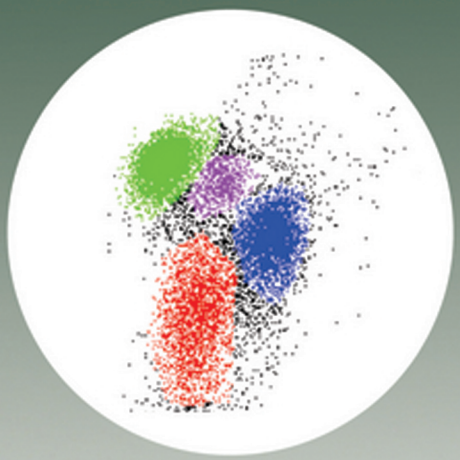

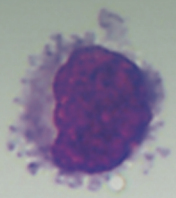

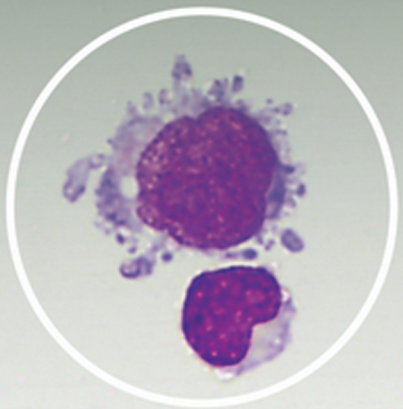

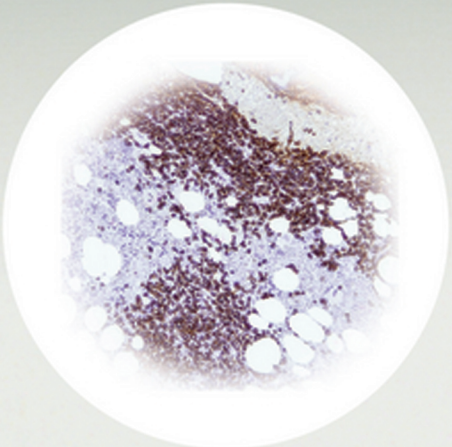

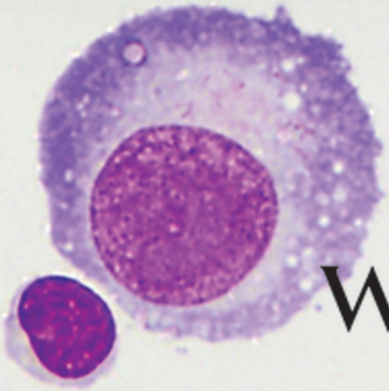

WILEY

Practical Flow Cytometry in Haematology: 100 Worked Examples

Practical Flow Cytometry in Haematology: 100 Worked Examples

Mike Leach FRCP, FRCPath
Consultant Haematologist and Honorary Senior Lecturer
Haematology Laboratories and West of Scotland Cancer Centre
Gartnavel General Hospital
Glasgow, UK

Mark Drummond PhD, FRCPath
Consultant Haematologist and Honorary Senior Lecturer
Haematology Laboratories and West of Scotland Cancer Centre
Gartnavel General Hospital
Glasgow, UK

Allyson Doig MSc, FIBMS
Haemato-Oncology Laboratory Manager
Haematology Laboratories
Gartnavel General Hospital
Glasgow, UK

Pam McKay
Consultant Haematologist
Haematology Laboratories and West of Scotland Cancer Centre
Gartnavel General Hospital
Glasgow, UK

Bob Jackson
Consultant Pathologist
Department of Pathology
Southern General Hospital
Glasgow, UK

Barbara J. Bain MBBS, FRACP, FRCPath
Professor of Diagnostic Haematology
St Mary's Hospital Campus of Imperial College
Faculty of Medicine, London
and Honorary Consultant Haematologist,
St Mary's Hospital, London, UK

WILEY Blackwell

This edition first published 2015 © 2015 by John Wiley & Sons, Ltd

Registered office: John Wiley & Sons, Ltd, The Atrium, Southern Gate, Chichester, West Sussex, PO19 8SQ, UK

Editorial offices: 9600 Garsington Road, Oxford, OX4 2DQ, UK
The Atrium, Southern Gate, Chichester, West Sussex, PO19 8SQ, UK
111 River Street, Hoboken, NJ 07030-5774, USA

For details of our global editorial offices, for customer services and for information about how to apply for permission to reuse the copyright material in this book please see our website at www.wiley.com/wiley-blackwell

Library of Congress Cataloging-in-Publication Data

Leach, Richard M. (Haematologist), author.
Practical flow cytometry in haematology : 100 worked examples / Mike Leach [and 5 others].
p. ; cm.
Includes index.
ISBN 978-1-118-74703-2 (hardback)
I. Title.
[DNLM: 1. Hematologic Diseases – diagnosis – Case Reports. 2. Hematologic Neoplasms – diagnosis – Case Reports. 3. Flow Cytometry – methods – Case Reports. 4. Hematology – methods – Case Reports. WH 120]
RC636
616.1′5075–dc23

2015007734

A catalogue record for this book is available from the British Library.

Wiley also publishes its books in a variety of electronic formats. Some content that appears in print may not be available in electronic books.

Set in 8.5/11pt, MinionPro by Laserwords Private Limited, Chennai, India

1 2015

Contents

Preface

In our first publication 'Practical Flow Cytometry in Haematology Diagnosis' we presented an outline approach to the use and applications of flow cytometric immunophenotyping in the diagnostic haematology laboratory. We showed how this technique could be used to study blood, bone marrow and tissue fluid samples in a variety of clinical scenarios to achieve a diagnosis, taking into account important features from the clinical history and examination alongside haematology, morphology, biochemistry, immunology, cytogenetic, histopathology and molecular data. This text was illustrated with a series of 'worked examples' from real clinical cases presenting to our institution. These cases have proven to be very popular and so a companion publication dedicated to 100 new 'worked examples' seemed justified and is presented here.

The principles used in the approach to each case are exactly the same as used in the first publication and cases are illustrated with tissue pathology and cytogenetic and molecular data, which are integrated to generate, where appropriate, a diagnosis based on the WHO Classification of Tumours of Haematopoietic and Lymphoid Tissues. We present a spectrum of clinical cases encountered in our department from both adult and paediatric patients and of course, if the title is to be justified, flow cytometry plays a role in every case. Furthermore, we present both neoplastic and reactive disorders and the cases appear in no particular order so that the reader should have no pre-conceived idea as to the nature of the diagnosis in any case. May–Grünwald–Giemsa (MGG)-stained films of peripheral blood and bone marrow aspirates are presented with flow cytometry data alongside haematoxylin and eosin (H&E)-stained bone marrow and tissue biopsy sections. Immunohistochemistry is used to further clarify the tissue lineage and cell differentiation. Cytogenetic studies using metaphase preparations are used to identify translocations and chromosome gains and losses whilst interphase fluorescence *in situ* hybridisation (FISH) studies and polymerase chain reaction (PCR) are used to identify gene fusions, break-aparts and deletions. The presentation is brought to a conclusion and the particular features that are important in making a diagnosis are highlighted and discussed. The cases are also listed according to disease classification toward the end (page 390) so that the text can also be used as a reference manual.

The analysis of blood, bone marrow and tissue fluid specimens requires a multi-faceted approach with the integration of scientific data from a number of disciplines. No single discipline can operate in isolation or errors will occur. Flow cytometry technology is in a privileged position in that it can provide rapid analysis of specimens; it is often the first definitive investigation to produce results and help formulate a working diagnosis. The results from flow cytometry can help to structure investigative algorithms to ensure that the appropriate histopathological, cytogenetic and molecular studies are performed in each case. Tissue samples are often limited in volume and difficult to acquire so it is important to stratify investigations accordingly and to get the most from the material available. It is not good scientific or economic practice to run a large series of poorly focussed analyses on every case. Appropriate studies need to be executed in defined circumstances and flow cytometry can guide subsequent investigations in a logical fashion. In some situations a rapid succinct diagnosis can be achieved; immunophenotyping excels in the identification of acute leukaemia. Cytogenetic studies and molecular data give important prognostic information in these patients. But of course the recognised genetic aberrations need to be demonstrated if the diagnosis is to be substantiated. Acute promyelocytic leukaemia can often be confidently diagnosed using morphology alongside immunophenotyping data, but a *PML* translocation to the *RARA* fusion partner, needs to be shown. Flow cytometry cannot operate in isolation; despite having the 'first bite of the cherry' the differential diagnosis can still be wide open. There are a good number of worked examples illustrated here where immunophenotyping was not able to indicate a specific diagnosis. The disease entities with anaplastic or 'minimalistic' phenotypes frequently cause difficulty. Appropriate histopathology and FISH, performed on the basis of flow cytometric findings, highlighting abnormal protein expression and gene rearrangement respectively, can make a major contribution to diagnosis and disease classification. Only when a specific

diagnosis is made and prognostic parameters are assessed can the optimal management plan be considered for each individual patient. Finally, the goal posts are constantly moving and developments in the molecular basis of disease, refining disease classification, are evolving rapidly. Whether we are considering eosinophilic proliferations, the myriad of myeloproliferative neoplasms, lymphoproliferative disorders or acute leukaemias we are constantly noting developments and adjusting diagnosis and prognosis accordingly. This is an era of evolving diagnostic challenge and rapid molecular evolution where the practising clinician needs to keep abreast of the significant developments in all areas of haematopathology.

The flow cytometric principles applied to each case have been described in detail in 'Practical Flow Cytometry in Haematology Diagnosis' and some working knowledge is required to interpret the cases described. We also anticipate a reasonable ability in morphological assessment and a capacity to identify morphological variations seen in various disease states. In spite of this we do endeavour to describe the diagnostic logic that we have applied to each worked example and demonstrate how cellular immunophenotypes have helped determine the nature of the disorder.

This text will be of interest to all practicing haematologists and to histopathologists with an interest in haematopathology but it is particularly directed at trainee haematologists and scientists preparing for FRCPath examinations.

Acknowledgement

We are grateful for the substantial assistance of Dr Avril Morris DipRCPath, Principal Clinical Scientist, West of Scotland Genetic Services, Southern General Hospital, Glasgow with regard to the provision of the cytogenetic data and images relevant to the clinical cases presented here.

List of Abbreviations

ADP	adenosine diphosphate
AITL	angioimmunoblastic T-cell lymphoma
AL	acute leukaemia
ALCL	anaplastic large cell lymphoma
ALL	acute lymphoblastic leukaemia
ALP	alkaline phosphatase
ALT	alanine transaminase
AML	acute myeloid leukaemia
AML-MRC	acute myeloid leukaemia with myelodysplasia-related changes
ANA	antinuclear antibody
APC	allophycocyanin
APL	acute promyelocytic leukaemia
APTT	activated partial thromboplastin time
ASM	aggressive systemic mastocytosis
AST	aspartate transaminase
ATLL	adult T-cell leukaemia/lymphoma
ATRA	all-*trans*-retinoic acid
AUL	acute undifferentiated leukaemia
B-ALL	B-lineage acute lymphoblastic leukaemia
BCLU	B-cell lymphoma, unclassifiable, with features intermediate between diffuse large B-cell lymphoma and Burkitt lymphoma
BEAM	carmustine (BCNU), etoposide, cytarabine (cytosine arabinoside) and melphalan
BL	Burkitt lymphoma
BP	blast phase
BPDCN	blastic plasmacytoid dendritic cell neoplasm
c	cytoplasmic
CD	cluster of differentiation
CHOP	cyclophosphamide, doxorubicin, vincristine and prednisolone
CLL	chronic lymphocytic leukaemia
CML	chronic myeloid leukaemia
CMML	chronic myelomonocytic leukaemia
CMV	cytomegalovirus
CNS	central nervous system
CODOX M/IVAC	cyclophosphamide, vincristine, doxorubicin, methotrexate/ ifosphamide, mesna, etoposide, cytarabine
CR	complete remission
CRAB	calcium (elevated), renal failure, anaemia, bone lesions
CSF	cerebrospinal fluid
CT	computed tomography
CTCL	cutaneous T-cell lymphoma
CTD	cyclophosphamide, thalidomide and dexamethasone
CXR	chest X-ray
cyt, cyto	cytoplasmic
DEXA scanning	dual energy X-ray absorptiometry scanning
DIC	disseminated intravascular coagulation
DKC	dyskeratosis congenita
DLBCL	diffuse large B-cell lymphoma
DM	double marking
EBER	EBV-encoded small RNAs
EBV	Epstein-Barr virus
EBV LMP	Epstein-Barr virus latent membrane protein
EDTA	ethylene diamine tetra-acetic acid
eGFR	estimated glomerular filtration rate
EMA	eosin-5-maleimide
EORTC	European Organization for Research and Treatment of Cancer
ESHAP	etoposide, methyl prednisolone, cytarabine, cisplatin
ESR	erythrocyte sedimentation rate

ET	essential thrombocythaemia
ETP-ALL	early T-cell precursor acute lymphoblastic leukaemia
FAB	French–American–British (leukaemia classification)
FBC	full blood count
FDG	fluorodeoxyglucose
FISH	fluorescence *in situ* hydridisation
FITC	fluorescein isothocyanate
FL	follicular lymphoma
FLAER	fluorescein-conjugated proaereolysin
FLAG	fludarabine, cytarabine, granulocyte colony-stimulating factor
FLAG-IDA	fludarabine, cytarabine, granulocyte colony-stimulating factor, idarubicin
FSC	forward scatter
GGT	gamma glutamyl transferase
GI	gastrointestinal
Gp	glycoprotein
GP	general practitioner
GPI	glycosylphosphatidylinositol
H&E	haematoxylin and eosin
Hb	haemoglobin concentration
HCL	hairy cell leukaemia
HCL-V	hairy cell leukaemia variant
HHV	human herpesvirus
HIV	human immunodeficiency virus
HL	Hodgkin lymphoma
HLA-DR	human leucocyte antigen DR
HS	hereditary spherocytosis
HTLV-1	human T-cell lymphotropic virus-1
ICC	immunocytochemistry
Ig	immunoglobulin
IgA	immunoglobulin A
IgG	immunoglobulin G
IgM	immunoglobulin M
IHC	immunohistochemistry
IPSS	International Prognostic Scoring System
ISCL	International Society for Cutaneous Lymphomas
ISH	in situ hybridisation
ISM	indolent systemic mastocytosis
ITD	internal tandem duplication
ITP	'idiopathic' (autoimmune) thrombocytopenia purpura
IVLBCL	intravascular large B-cell lymphoma
LAP	leukaemia-associated phenotype
LBL	lymphoblastic lymphoma
LDH	lactate dehydrogenase
LFTs	liver function tests
LGL	large granular lymphocyte
LPD	lymphoproliferative disorder
MCH	mean cell haemoglobin
MCL	mantle cell lymphoma
MCV	mean cell volume
MDS	myelodysplastic syndrome/s
MDS/MPN	myelodysplastic/myeloproliferative neoplasm
MF	mycosis fungoides
MGG	May–Grünwald–Giemsa
MGUS	monoclonal gammopathy of undetermined significance
MM	multiple myeloma
mod	moderate fluorescence
MPAL	mixed phenotype acute leukaemia
MPN	myeloproliferative neoplasm
MPO	myeloperoxidase
MRD	minimal residual disease
MRI	magnetic resonance imaging
MZL	marginal zone lymphoma
NLPHL	nodular lymphocyte-predominant Hodgkin lymphoma
NOS	not otherwise specified
NR	normal range
PAS	periodic acid-Schiff
PCR	polymerase chain reaction
PD-1	an antigen, programmed death 1(CD279)
PE	phycoerythrin
PEL	primary effusion lymphoma
PET	positron-emission tomography
Ph	Philadelphia (chromosome)
PMF	primary myelofibrosis
PNET	primitive neuroectodermal tumour
PNH	paroxysmal nocturnal haemoglobinuria
PRCA	pure red cell aplasia
PT	prothrombin time
PTCL-NOS	peripheral T-cell lymphoma, not otherwise specified
PTLD	post-transplant lymphoproliferative disorder
PV	polycythaemia vera
RBC	red blood cell (count)
R-CHOP	rituximab, doxorubicin, vincristine and prednisolone
R-CVP	rituximab, cyclophosphamide, vincristine and prednisolone
RNA	ribonucleic acid
RQ-PCR	real-time quantitative polymerase chain reaction
RS	Reed–Sternberg

RT-PCR	reverse transcriptase polymerase chain reaction
SAA	severe aplastic anaemia
Sig	surface membrane immunoglobulin
SLE	systemic lupus erythematosus
SM	systemic mastocytosis
SM-AHNMD	systemic mastocytosis with associated clonal haematological non-mast cell disease
SMILE	dexamethasone, methotrexate, ifosfamide, L-asparaginase and etoposide
SSC	side scatter
T-ALL	T-lineage acute lymphoblastic leukaemia
TBI	total body irradiation
TdT	terminal deoxynucleotidyl transferase
TIA	T-cell intracellular antigen
TKI	tyrosine kinase inhibitor
T-LBL	T-lymphoblastic lymphoma
t-MDS	therapy-related myelodysplastic syndrome
TRAP	tartrate-resistant acid phosphatase
TT	thrombin time
TTP	thrombotic thrombocytopenic purpura
U&Es	urea, electrolytes and creatinine
USS	ultrasound
WAS	Wiskott–Aldrich syndrome
WASp	Wiskott–Aldrich syndrome protein
WBC	white blood cell (count)
WM	Waldenström macroglobulinaemia

Technical Notes

The patients presented in 100 Worked Examples were all real cases encountered and investigated in a regional flow cytometry laboratory serving a population of approximately 2.5 million over a period of 18 months. These are individually presented with a history that reflects the actual events for each patient, commencing with the presenting clinical features and the initial basic laboratory tests and then proceeding to flow cytometry, bone marrow aspirate morphology, bone marrow trephine biopsy histology with immunohistochemistry studies and other specialised cytogenetic and molecular analyses.

Full blood counts

The full blood counts and marrow counts (for appropriate dilutions in relation to antibody) were performed on a Sysmex XN analyser. The differential leucocyte counts are automated counts from the analyser. It should be noted that sometimes, in an automated count, abnormal cells are misidentified and the leucocyte sub-populations differ from a manual differential performed on a blood film. Such misidentifications are indicated by inverted commas.

Biochemistry and immunology studies

All relevant biochemistry and immunology data is given in relation to the context of each patient presentation and in terms of investigations that were thought to be relevant to the case as the clinical diagnosis evolved. Some retrospectively relevant data may be missing but this reflects the true nature of these actual patient scenarios and the investigations that were considered necessary at that time. Serum calcium values given are all corrected in accordance with serum albumin level.

Flow cytometry analysis

Flow cytometry studies were all performed using a Becton Dickinson FACS Canto II analyser. The findings are presented as a list of positive and negative results in relation to the antigen and target cell population and the gating strategies applied to each case are explained. A series of scatter plots and histograms are presented to illustrate specific informative points. The expression of most membrane antigens is graded as positive when more than 20% of gated events are positive; the exceptions being CD34, CD117 and cytoplasmic antigens where a threshold of 10% has been used. Where the percentage positivity for a given membrane antigen in the gated target population is borderline positive so that some cells appear negative and some positive we have used the term 'partial' to describe antigen expression. Cytoplasmic expression of an antigen is indicated with the prefix 'c' (cytoplasmic expression of CD3 being cCD3) but on some scatter plots 'cyt' or 'cyto' has been used. The intensity of antigen expression in terms of median fluorescence intensity is graded as dim, moderate or bright compared to our laboratory reference ranges for normal cells of each relevant lineage. See Figures 1.1a–g for a schematic representation of these principles.

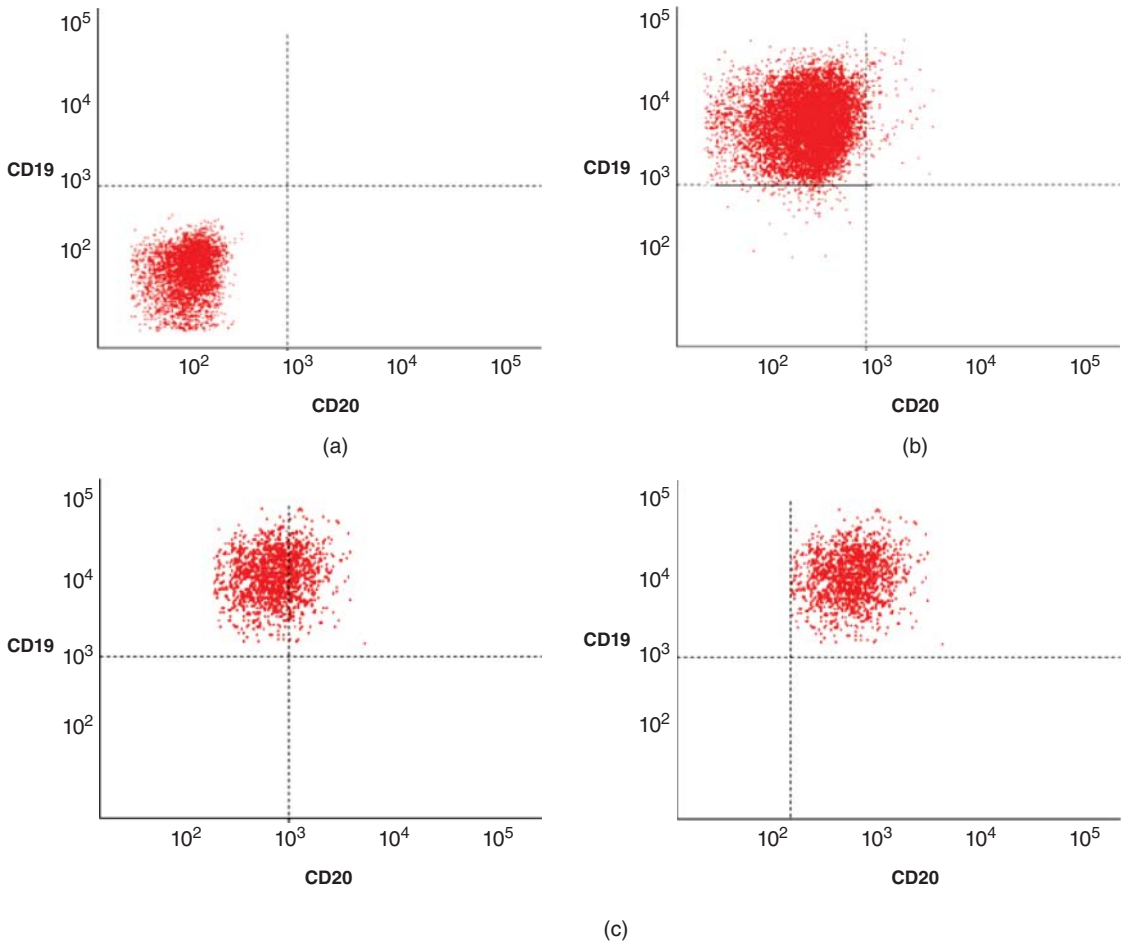

Figure 1.1 Visual representation of strength of fluorescence in flow cytometry (not actual patient specimens), showing an isotype control and eight CD19-positive samples which show fluorescence intensity with CD20 varying from negative to bright. (a) Isotype control, used to set thresholds. (b) Negative (consistent with a CD19-positive, CD20-negative B-cell precursor neoplasm). (c) Partial positive, indicating that CD20 antigen expression varies from negative to positive (consistent with a precursor B-cell neoplasm). (c adjusted) Indicating that the threshold for positivity might be reduced by the cytometrist where a discrete dim positive population is identified. (d) Dim CD20 antigen expression (consistent with chronic lymphocytic leukaemia). (e) Moderate intensity, indicating medium strength of CD20 antigen expression (consistent with B-cell non-Hodgkin lymphoma). (f) bright, indicating strong CD20 antigen expression (consistent with hairy cell leukaemia). (g) Two distinct populations, one partial and dim and one bright (could indicate two unrelated B-lineage neoplasms or transformation of a low grade lymphoma). (h) Contrasting with (g), a heterogeneous single population with fluorescence intensity varying from negative to moderate with a minority being bright.

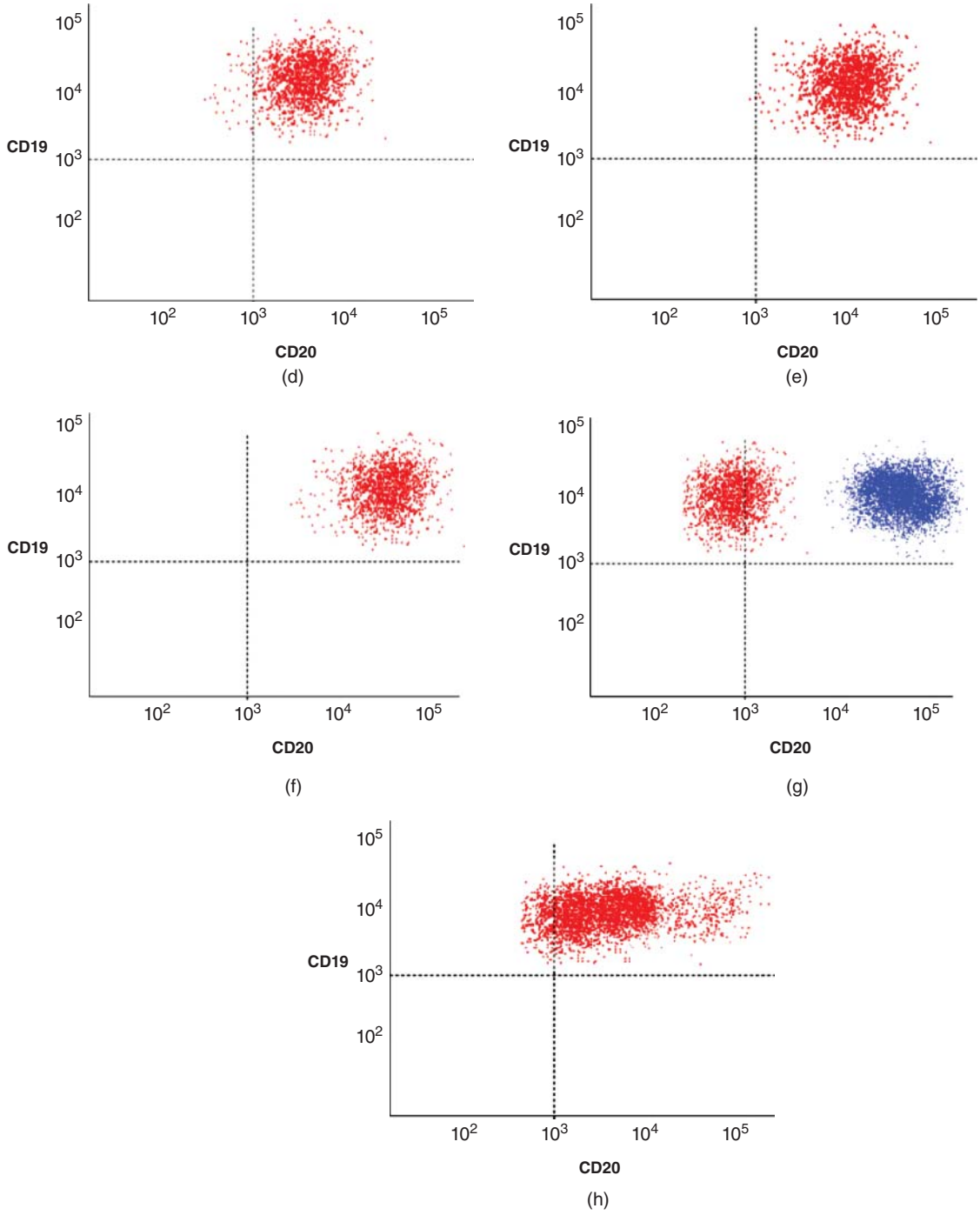

Figure 1.1 (*Continued*)

Immunohistochemistry in paraffin-embedded formalin fixed tissue

In the following section a list is presented of the immunohistochemical reagents used in assessing the paraffin embedded material (bone marrow trephine and lymph node biopsies) in the worked examples described. It should be pointed out that specificities and sensitivities may differ from the antibodies used in flow cytometry due to the effects of formalin fixation and decalcification resulting in antigen loss or masking. For example, CD5 may be detected by flow cytometry in a peripheral blood B-cell lymphocytosis but immunocytochemistry may on occasion be negative for the same marker in the trephine specimen. CD56 is aberrantly expressed by plasma cells in myeloma yet immunoreactivity for this antibody within plasma cells in paraffin sections is seen in only a minority of cases. The opposite situation may also occur where an antigen such as TdT is strongly positive by immunohistochemistry on the fixed tissue but is negative on the flow sample. Reticulin fibrosis is reported as per the WHO classification as grade 0, 1, 2 or 3.

These specific features of different techniques need to be appreciated when formulating the combined pathology report and an understanding of the strengths and weaknesses of each approach is essential when establishing a final diagnosis. Cytogenetic and molecular studies have a major influence on disease classification. Specific findings can carry diagnostic significance way in excess of any other single investigative modality e.g. *BCR-ABL1*, *PML-RARA*, *FIP1L1-PDGRFA*. Metaphase cytogenetic studies not infrequently fail, either reflecting the quality of the specimen or the disease entity being studied. Informed FISH and PCR studies can carry great diagnostic importance in certain clinical circumstances and molecular diagnostics will continue to inform disease classification with increasing power and specificity over the decades ahead.

Laboratory Values

Abbreviations and Normal Ranges.

Blood	
Haematology	
Haemoglobin concentration (Hb)	130–180 g/L (M) 125–170 g/L (F)
Mean cell volume (MCV)	80–100 fl
Reticulocyte count	50–100 $\times 10^9$/L
White blood cell count (WBC)	4–11 $\times 10^9$/L
Neutrophils	2–7 $\times 10^9$/L
Lymphocytes	1.5–4 $\times 10^9$/L
Monocytes	0.2–0.8 $\times 10^9$/L
Eosinophils	0.04–0.4 $\times 10^9$/L
Basophils	0.01–0.1 $\times 10^9$/L
Haematinics	
Serum ferritin	10–275 ng/mL
Serum folate	3.1–20 ng/mL
Serum vitamin B_{12}	200–900 pg/mL
Coagulation	
Prothrombin time (PT)	9–13 s
Activated partial thromboplastin time (APTT)	27–38 s
Thrombin time (TT)	11–15 s
Fibrinogen	1.5–4 g/L
D dimer	0–243 ng/mL
Biochemistry	
Sodium (Na)	135–145 mmol/L
Potassium (K)	3.5–5.0 mmol/L
Urea	2.5–7.5 mmol/L
Creatinine	40–130 μmol/L
Bicarbonate	20–30 mmol/L

Blood	
Urate	0.2–0.43 mmol/L
Lactate	<2.4 mmol/L
Lactate dehydrogenase (LDH)	80–240 U/L
Aspartate transaminase (AST)	<40 U/L
Alanine transaminase (ALT)	<50 U/L
Gamma glutamyl transferase (GGT)	<70 U/L
Alkaline phosphatase (ALP)	40–150 U/L
Calcium adjusted	2.1–2.6 mmol/L
Phosphate	0.7–1.4 mmol/L
C-reactive protein (CRP)	<10 mg/L
Bilirubin	<20 μmol/L
Albumin	32–45 g/L
Globulins	23–38 g/L
Serum osmolality	270–295 mmol/kg
Urine protein/creatinine ratio	0–15 mg/mmol
Immunoglobulin G (IgG)	6–16 g/L
Immunoglobulin A (IgA)	0.8–4.0 g/L
Immunoglobulin M (IgM)	0.5–2.0 g/L
Serum free light chains	
Free kappa	3.3–19.4 mg/L
Free lambda	5.7–26.3 mg/L
Cerebrospinal fluid (CSF)	
Protein	<0.4 g/L
Cells	<0.001 $\times 10^9$/L (<10 cells/μL)
Glucose	2 mmol/L less than serum glucose

1 Case 1

An 11-year-old boy was admitted with a short history of fever, sweats, dyspnoea and left chest discomfort. There was no past history of note. Examination identified features of a left pleural effusion. There was also a tender swelling of the left anterior chest in the upper pectoral region and palpable cervical lymphadenopathy. The liver and spleen were not palpable.

Laboratory investigations

FBC and blood film: normal

U&Es, LFTs: normal. LDH was 1460 U/L.

Imaging

The CXR showed opacification and loss of aeration of the left hemithorax in keeping with a pleural effusion (Figure 1.1).

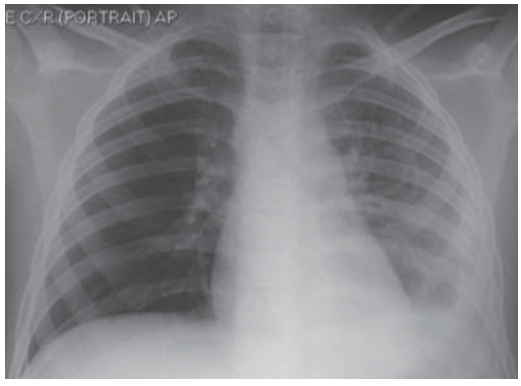

Figure 1.1 CXR.

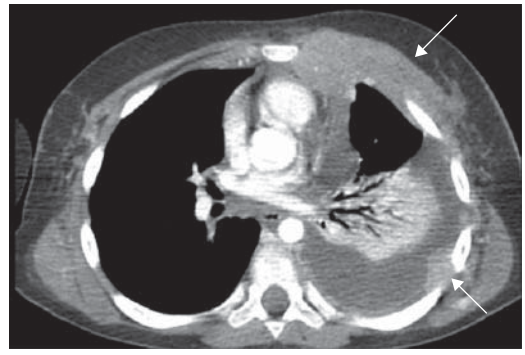

Figure 1.2 CT.

CT imaging confirmed this but in addition identified a left pleural-based mass, abnormal soft tissue in the left pectoral muscles (arrows, Figure 1.2) and cervical lymphadenopathy. In addition, there was collapse/consolidation of the lower left lung, creating the appearance of an air bronchogram. A core biopsy of a cervical node was taken and the pleural effusion was aspirated for analysis.

Flow cytometry

The pleural fluid cell count was 0.98×10^9/L. A cytospin preparation showed three distinct cell types: a small mature lymphoid population in keeping with reactive lymphocytes, an intermediate sized/large sized lymphoid population and a large cell population with pleomorphic morphology and blue cytoplasm (Figures 1.3 – 1.6). The cells with the abundant cytoplasm (Figures 1.3 and 1.4) and the single binucleate cell (Figure 1.6) are reactive mesothelial cells. The cells with the cytoplasmic blebs (Figures 1.4 – 1.6) are the disease cells,

Practical Flow Cytometry in Haematology: 100 Worked Examples, First Edition. Mike Leach, Mark Drummond, Allyson Doig, Pam McKay, Bob Jackson and Barbara J. Bain.

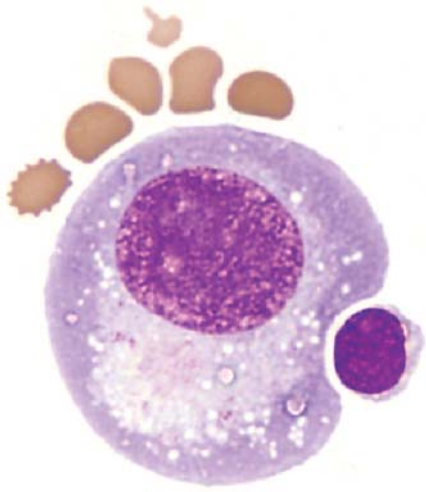

Figure 1.3 MGG, ×500.

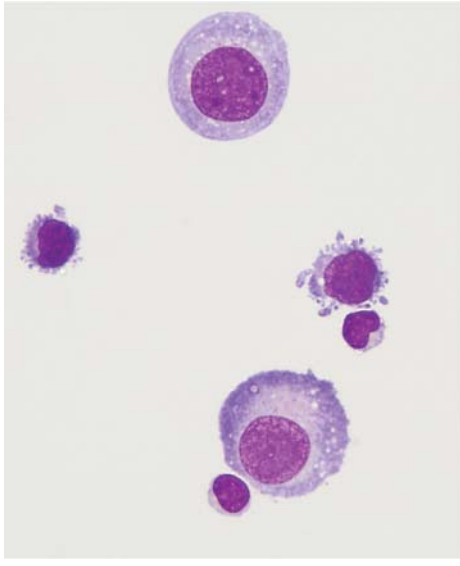

Figure 1.4 MGG, ×500.

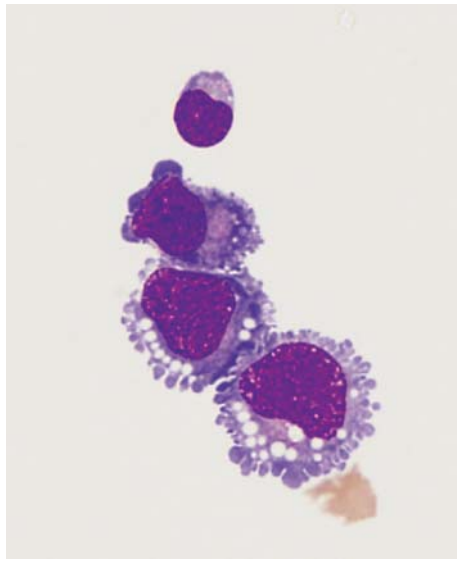

Figure 1.5 MGG, ×500.

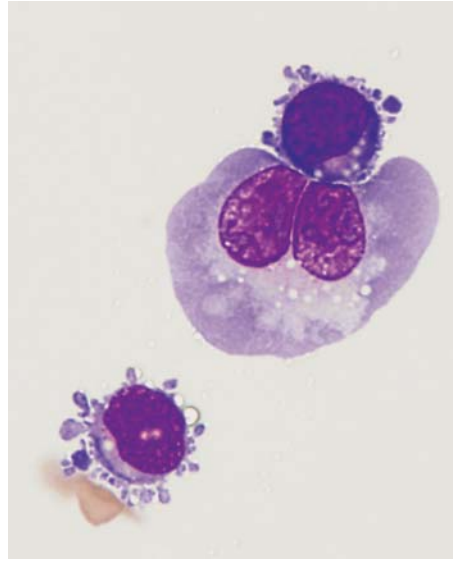

Figure 1.6 MGG, ×500.

which were the subsequent focus for immunophenotyping studies.

By applying a blast gate to the suspected malignant cells in the FSC/SSC analysis (Figure 1.7), they were shown to express CD45^{bright} (Figure 1.8), CD2 (Figure 1.9), cCD3 [whilst surface CD3 was negative apart from a few reactive T cells (Figure 1.8)], partial CD7 (Figure 1.10) and CD13. Other T-lineage markers were negative.

This is therefore a T-lymphoid neoplasm, indicated by positivity for cCD3 expression, with limited lineage-specific

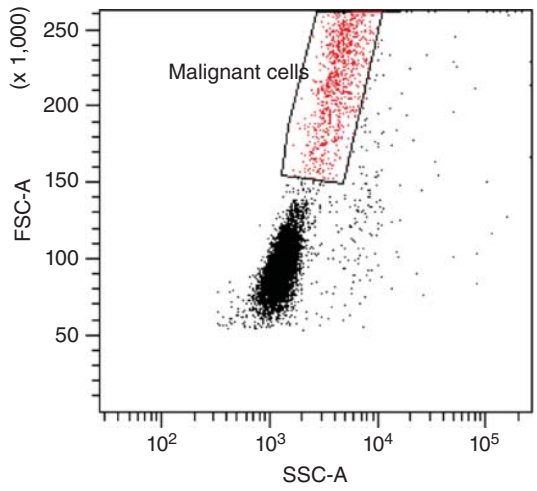

Figure 1.7 FSC/SSC.

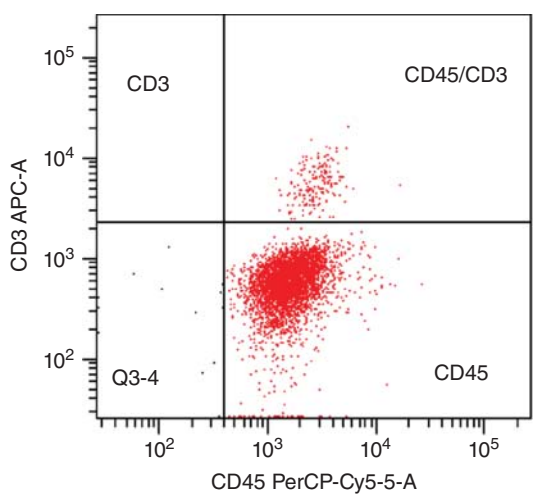

Figure 1.8 CD3/CD45.

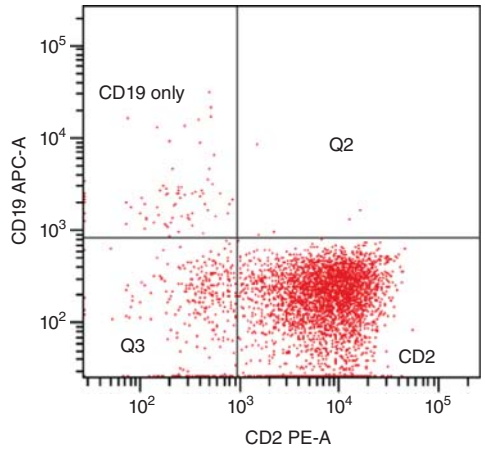

Figure 1.9 CD2/CD19.

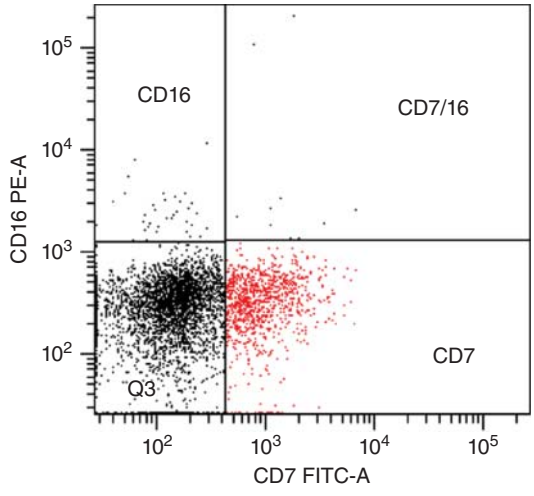

Figure 1.10 CD7/CD16.

markers and an aberrant myeloid marker. The tumour has medium sized/large cell morphology. It was showing aggressive clinical behaviour with extranodal tissue invasion in this 11-year-old patient. An anaplastic large cell lymphoma had to be considered and the medium sized/large cells in the pleural fluid were shown to be strongly expressing CD30 (not shown).

Histopathology

An H&E-stained core biopsy of a cervical node is shown in Figure 1.11. The node is replaced by an infiltrate of undifferentiated pleomorphic large cells with prominent nucleoli.

Immunohistochemistry showed the large cells to express CD45, epithelial membrane antigen (EMA), CD2 focally (Figure 1.12), CD7, granzyme B and CD30 (Figure 1.13). In addition, there was strong nuclear and cytoplasmic staining for anaplastic lymphoma kinase (ALK) protein (Figure 1.14).

The CD30 staining was particularly useful in demonstrating lymphatic invasion within the capsule of the node (Figure 1.15).

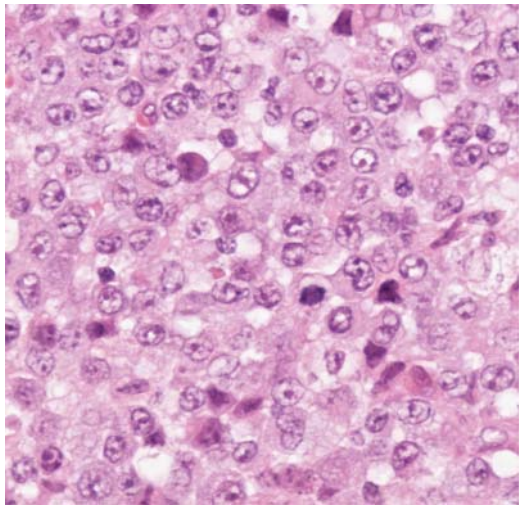

Figure 1.11 H&E, ×400.

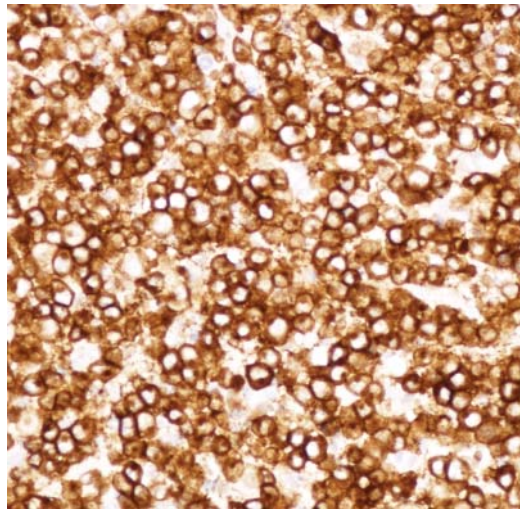

Figure 1.13 CD30, ×400.

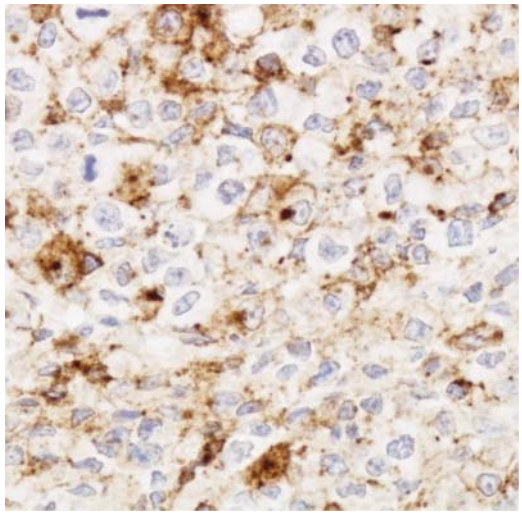

Figure 1.12 CD2, ×400.

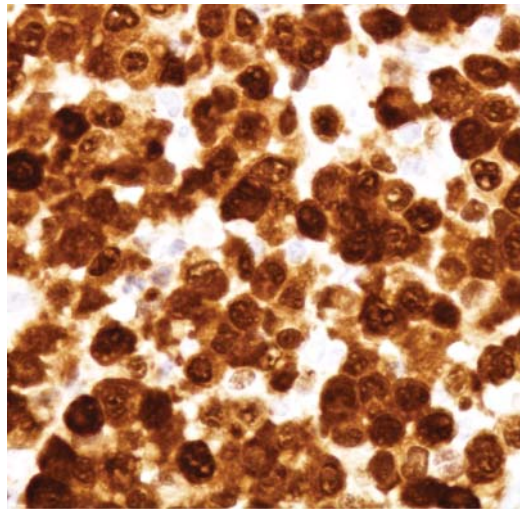

Figure 1.14 ALK, ×400.

FISH studies

A t(2;5)(p23;q35) translocation, rearranging the *ALK* and *NPM1* (nucleophosmin) genes, was shown by FISH studies on paraffin-embedded lymph node tissue. The presence of this specific translocation is highly associated with both nuclear and cytoplasmic positivity for ALK.

Discussion

Anaplastic large cell lymphoma (ALCL) is an aggressive mature T-cell neoplasm with pleomorphic, often large cell, morphology. It frequently fails to show surface expression of T-lineage-specific markers and to potentially further mislead may express aberrant myeloid antigens. This is an

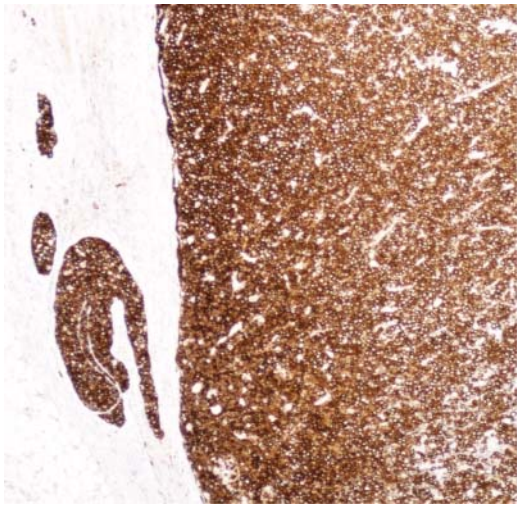

Figure 1.15 CD30, ×100.

important condition to recognise; it frequently shows rapid progression with extranodal tissue involvement and it can rarely appear in the blood. Treatment of ALK^+ ALCL is usually rewarding, particularly in paediatric patients, with prompt response to chemotherapy and frequent durable remissions.

Final diagnosis

Anaplastic large cell lymphoma (ALK^+)

2 Case 2

A 72-year-old woman presented with a few months' history of fatigue and the more recent onset of breathlessness and night sweats. On clinical examination she had a large right-sided pleural effusion but no palpable lymphadenopathy.

Laboratory results

FBC: Hb 158 g/L, WBC 16.6 × 10^9/L (neutrophilia and monocytosis) and platelets 502 × 10^9/L.

U&Es: normal. LFTs were mildly deranged (ALT 52 U/L, alkaline phosphatase 173 U/L). Albumin was low at 29 g/L and serum LDH was raised at 584 U/L.

Imaging

A CT scan demonstrated a large right-sided pleural effusion with collapse of the right middle and lower lobes and partial collapse of the upper lobe (Figure 2.1). In addition, there were large volume, confluent, necrotic nodal masses in the right hilar, mediastinal, retrocrural, paracardiac and para-aortic areas (not shown) as well as pleural deposits (arrow, Figure 2.1).

Pleural fluid biochemistry and cytology

The pleural fluid LDH was markedly elevated at 2171 U/L with relatively low glucose at 7.2 mmol/L (patient diabetic) and protein of 43 g/L.

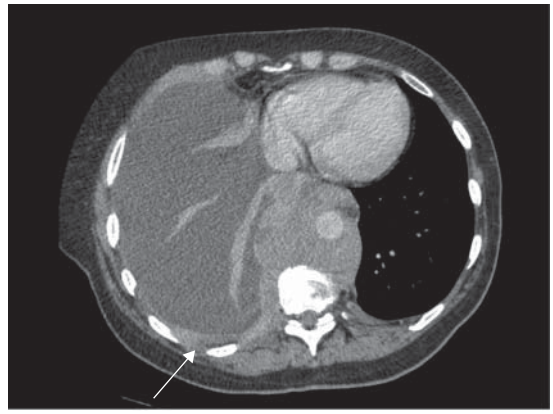

Figure 2.1 CT.

Microscopy of the pleural fluid showed lymphoid cells admixed with neutrophils, histiocytes and mesothelial cells. Most of the lymphoid cells were small but an admixed population of medium-sized cells with slightly irregular nuclei was also present. On morphology alone, the lymphoid cells were thought likely to be reactive but the reporting pathologist suggested that a fresh pleural fluid specimen should be assessed using flow cytometry.

Morphology (pleural fluid)

A specimen of pleural fluid was received by our laboratory. The WBC was found to be 6.3 × 10^9/L. A cytospin preparation showed a cellular specimen with notable macrophages, neutrophils and small lymphocytes. In addition, some large blastoid lymphoid cells were seen (Figures 2.2 – 2.5).

Practical Flow Cytometry in Haematology: 100 Worked Examples, First Edition. Mike Leach, Mark Drummond, Allyson Doig, Pam McKay, Bob Jackson and Barbara J. Bain.

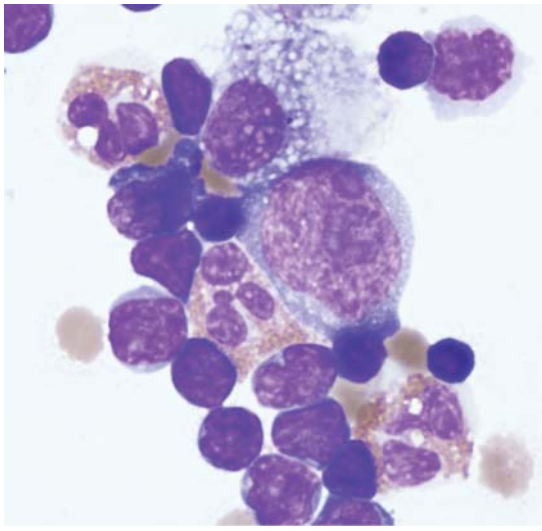

Figure 2.2 MGG, ×500.

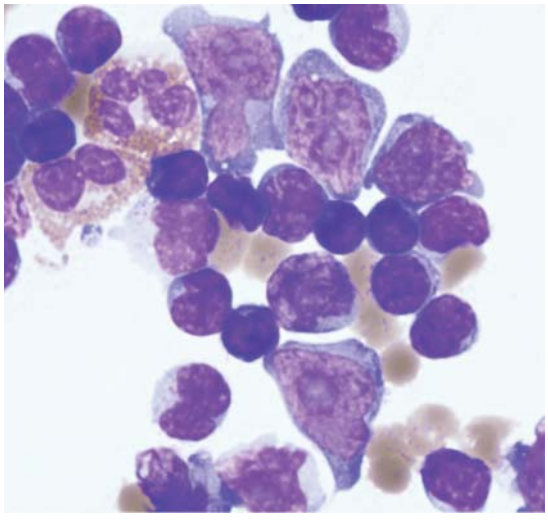

Figure 2.3 MGG, ×500.

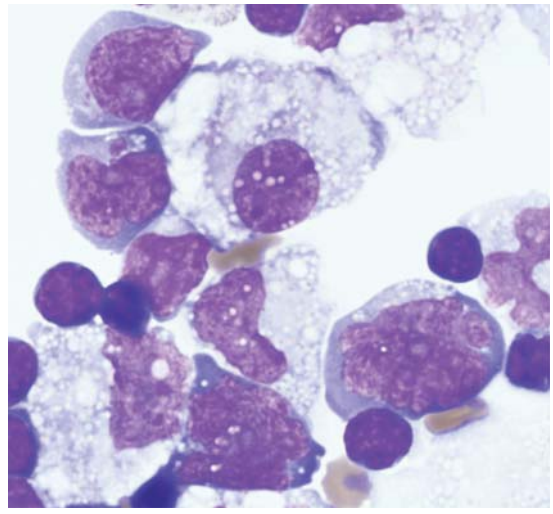

Figure 2.4 MGG, ×500.

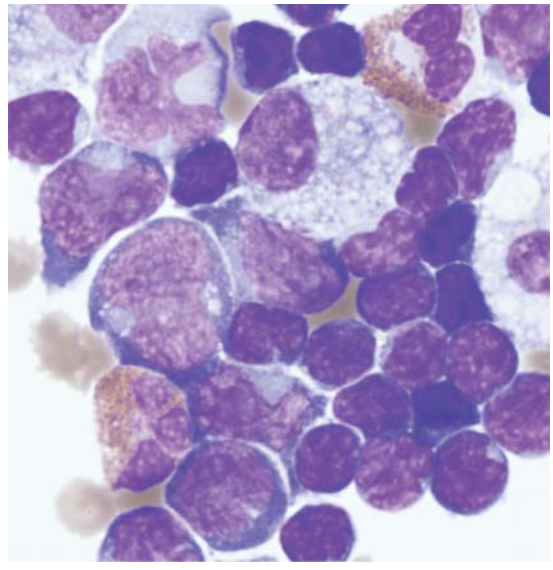

Figure 2.5 MGG, ×500.

Flow cytometry (pleural fluid)

The FSC/SSC plot shows the orientation of the different populations of cells described above. The small lymphoid population (Figure 2.6) comprised mainly reactive T cells (black events with mixture of $CD4^+$ and $CD8^+$ cells) and normal B cells (blue events). Seventeen per cent of all leucocytes were $CD19^+$ B cells (Figure 2.7) showing a mature pan-B phenotype with CD20 positivity and a hint of monoclonality (kappa 73%, lambda 18%). The SSC analysis in Figure 2.7, however, defines 2 B-cell populations with different scatter characteristics, populations P1 and P2.

By gating on the higher SSC profile B cells (P2 red events, Figure 2.7, which are larger indicated by high FSC in Figure 2.6), a clear clonal population was demonstrated showing strong CD20 positivity, expression of CD10/HLA-DR (Figure 2.8), CD38, FMC7, CD79b and CD22 with kappa light chain restriction (Figure 2.9).

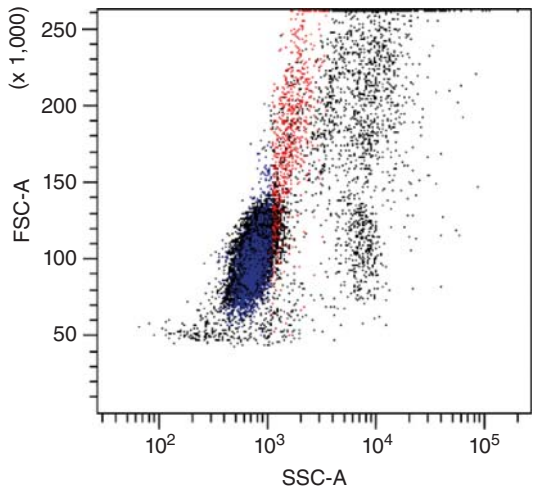

Figure 2.6 FSC/SSC.

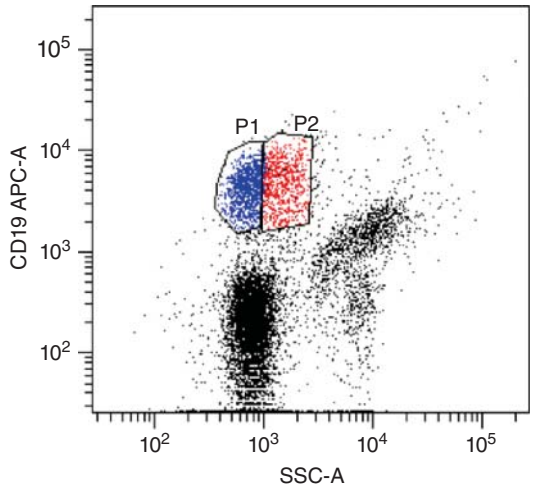

Figure 2.7 CD19/SSC.

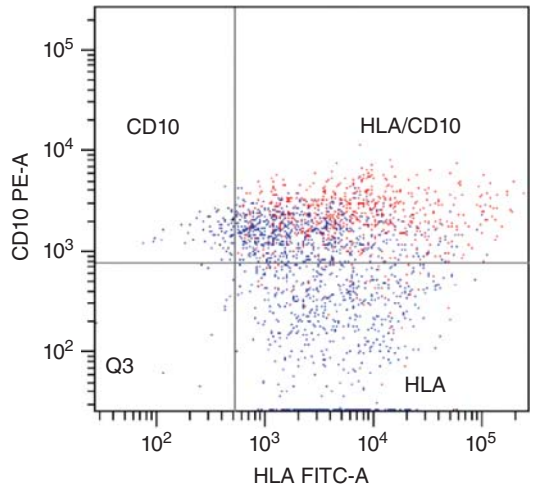

Figure 2.8 CD10/HLA-DR.

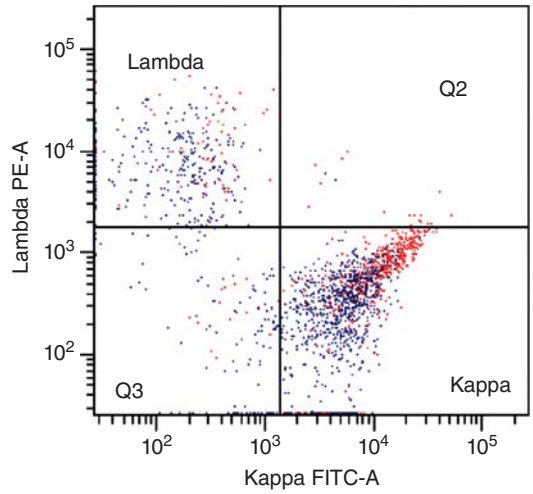

Figure 2.9 Kappa/lambda.

Note the phenotype of the blue events, population P1, representing residual small polyclonal reactive B cells.

Lymph node biopsy

A CT-guided core biopsy of a paravertebral node showed lymphoid infiltration by predominantly small centrocytic cells with occasional larger centroblasts. The cells were positive for CD20, CD10, BCL6 and BCL2 and negative for CD3, CD5, cyclin D1, CD23, CD43 and CD21. The proliferation fraction was low (~10%). The histological and immunohistochemical appearances were in keeping with follicular lymphoma, grade 2, with no evidence of high-grade transformation. FISH for the t(14;18) translocation was positive.

Bone marrow aspirate and trephine biopsy

These were both normal.

Discussion

The clinical presentation, imaging, pleural fluid morphology and flow cytometry were most in keeping with a diagnosis of an aggressive, mature $CD10^+$ B-cell neoplasm. Diffuse large